PROCEEDINGS OF SCIENCE

HI emission and absorption diagnostics

Raffaella Morganti
Netherlands Foundation for Research in Astronomy
Postbus 2, 7990 AA Dwingeloo (NL)
and
Kapteyn Astronomical Institute, University of Groningen,
PO Box 800, 9700 AV Groningen (NL)
E-mail: morganti@astron.nl

Hydrogen is the most common element in the Universe and is a powerful diagnostics for the kinematics and the conditions of the interstellar medium in galaxies. It provides key information on formation and evolution of galaxies, dark matter content and, for radio loud objects, on the conditions around the super massive black hole. Future radio telescopes, and in particular SKA, will use HI observations to solve some of the fundamental questions in astronomy.

This paper presents an overview of 21-cm HI observations. This goes from the parameters that need to be setup, how carry out the observations to the data reduction and visualization. The paper also briefly presents a few recent results on extragalactic HI studies. These results can be taken as examples of how important is to improve the sensitivity of HI observations. The still open questions associated to HI extragalactic studies are among the one driving the designs of the new SKA pathfinders, and ultimately, of SKA. The need for improved sensitivity but also for large field of view – with focal plane array or aperture arrays –is discussed.

The First MCCT-SKADS Training School
Medicina, Bologna Italy
September 23th- 29th 2007

PoS(MCCT-SKADS)012

1. Introduction

Hydrogen is the most abundant element in the Universe. It represents the main fuel for star formation and it can be used as tracer of the evolutionary stage of gas-rich galaxies and of the effects of their environments. The best way to detect the presence of neutral hydrogen (HI) is by its 21-cm emission line. The role of radio telescopes in, therefore, essential in order to image the distribution and kinematics of this gas in the Universe. Only when the state and distribution of this essential component will be known, the full picture e.g. of star formation history of the Universe will be completely understood. All this is to stress how important the study of HI is not only for what we have learned so far (see Sec. 4 for some examples) but also for answering some of the key open questions in astronomy.

Thus, it is not a by accident that the Square Kilometer Array (SKA) in its original idea - in the early 1990s - had as primary goal to be the telescope that would provide two orders of magnitude increase in collecting area (compared to existing radio telescopes) allowing the study of the neutral hydrogen content of galaxies to cosmologically significant distances (i.e. to z~2, compared with the z~0.2 possible with present day radio telescopes). Although the science case of SKA has now greatly expanded, HI still plays a key role in two of the key science projects of SKA: *Galaxy evolution and cosmology* and *Probing the dark ages.* In addition to this, and while working toward SKA and the SKA pathfinders, the existing telescopes are still providing new exciting results on the neutral hydrogen in the nearby Universe and just few examples of them will be discussed in Sec. 4.

This lecture aims at providing an overview of some basic concepts about HI 21-cm observations as well as an overview of some of the science that can be done using these diagnostics. A detailed description of the theory behind neutral hydrogen emission and details about the techniques for radio observations is available in a number of books (e.g. [7],[9],[13]). Therefore here I will only mention the most important parts/formulae.

The neutral hydrogen atom consists of 1 proton and 1 electron. The spin of the proton and electron can have only two orientations; spin axes parallel or anti-parallel. Although a rare event, the ground state of hydrogen atoms can undergo a hyperfine transition, and reverse the spin of the electron: the higher energy state is obtained when the spin of electron and proton are parallel. The difference in energy (6×10^{-6} eV) corresponds to a frequency of the transition of 1420.405752 MHz (21.105 cm). The temperature T_{spin} (spin or excitation temperature) accounts for the distribution of the atoms between the two states. The population of the two states is determined primarily by collisions between atoms. In other words, T_{spin} is equal to the kinetic temperature (but there are exceptions to this). These theories and some of the formulae described below are summarised in, among others, Verschuur (1974).

The 21-cm HI line was predicted by van de Hulst (1944) and later confirmed by observations (US, Australian & Dutch teams). The probability of a spontaneous transition is very small, 2.85×10^{-15} sec^{-1} (or 1 event per atom per 11 million years!) this rate increases to one transition per 400 years due to collisions. Despite of this, we can detect atomic hrydrogen

thanks to the fact that is the most common element in the universe. The HI line has an extremely small natural width: for a temperature of the gas of 100 K the width of the line is ~ 1 km sec^{-1} the observed lines are always much larger. Most of the commonly observed broadening is, therefore, due to Doppler shifts caused by the motion of the emitting regions relative to the observer. This means that this line is a powerful tracer of the gas kinematics.

1.1 HI emission

The derivation of all the formulae can be found in many books (see e.g. [9], [13]). I summarise here only few formulae of interest for the calculations that we will see later in this paper. Radio observations measure the T_B brightness temperature: temperature of an equivalent black body that will give the same power $T_B(\nu)=T_{spin}[1-e^{-\tau(\upsilon)}]$ where τ represents the optical depth. The column density of HI (i.e. the number of hydrogen atoms in a cylinder of unit cross-section, in the low optical depth limit) is $N_H = 1.82\cdot10^{18} \int T_B dV$. In term of observables, this formula can be turned into: $3.1\cdot10^{17}\ SdV/\theta^2$ where θ is beam size (arcmin), dV km s^{-1} and S is the observed flux in mJy beam^{-1}.

To derive the mass of the HI detected in emission we can use the formula: $M_{HI} = 2.365\cdot10^5 D^2 F \quad (M_{sun})$ where $F \sim \int S\, dV$ Jy km s^{-1} (1 Jy = 10^{-26} W/m^2/Hz) and D is the distance of the object in Mpc (with D ~ cz/H_0).

Typical values for column densities detected in emission range between a few x 10^{19} to up to 10^{21} cm^{-2} for a disk of an HI-rich spiral galaxy. In absorption, column densities of 10^{19} cm^{-2} are quite commonly seen against the nuclei of radio galaxies.

1.2 HI absorption

HI absorption can be detected when the neutral hydrogen is located in front of a radio continuum source. In this case we do not measure the T_B of the emission gas but the absorbed flux. The optical depth can be derived from $\Delta S = S_{cont}\, c_f\, (1-e^{-\tau})$ where ΔS is the absorbed flux, S_{cont} the flux of the continuum and c_f the covering factor (usually taken as 1).

The column density can be derived from $N_H = 1.823\cdot10^{18} T_{spin} \int \tau dv$ where T_{spin} accounts for the electrons those are in the upper state (i.e. those that do not absorb). The higher the T_{spin}, the more electrons are in the upper state and the higher column density is. From galactic studies, a typical value is T_{spin}= 100 K. However, we know that this is not always the case. For example, the presence of a strong continuum source near the H I gas may significantly increase the spin temperature (up to few thousand K) because in this case the radiative excitation of the HI hyperfine state can dominate the, usually more important, collisional excitation (see e.g., [1]).

2. Parameters of the HI observations

Spectral line 21-cm HI observations are carried out like normal radio observations with the additional need to specify the central frequency, the width of the observing band and the number of channels to provide the necessary velocity resolution. Fig. 1 shows a cartoon with these parameters listed. Actually, continuum observations in many radio telescopes are now carried out in spectral line mode to be able to obtain a large field of view (see contribution of Tom Muxlow these Proceedings) without being affected by beam smearing, make use of the band for a better uv coverage and be able to perform a better rejection/flagging of radio interferences.

In order to plan line observations one needs to define:

1. Redshift/velocity of the target: *central frequency*
2. Expected kinematics of the HI: *bandwidth*
3. Velocity resolution requested: *number of channels*
4. *Sensitivity* needed, depending on the redshift of the target
5. *Spatial resolution* and expected column density to be detected

The choice of some of these parameters depends on the type of objects to be studied and the goal of the observations. Some examples are considered below.

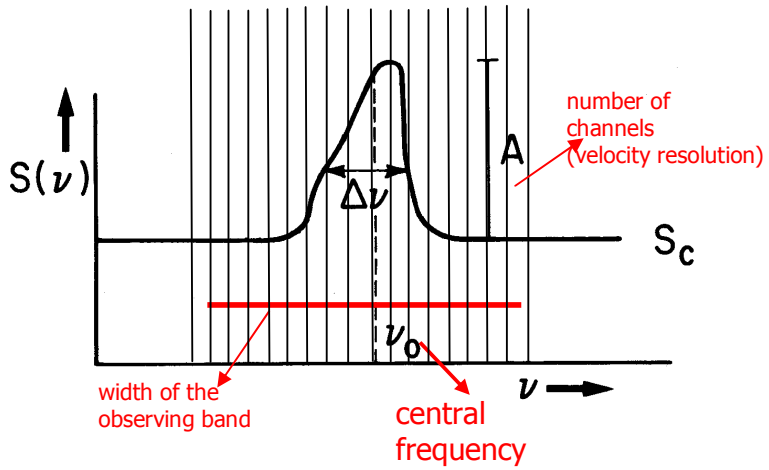

Figure 1- A cartoon showing the setup for line observations (modified from Roelfema 1994).

2.1 Central frequency

Choosing the central frequency may require more attention that one may expect. In order to be sure that the desired spectral line is in the desired channel inside the observed band, the velocity *and* rest frame of the target need to be specified (see e.g. [8], [14]). The observing frequency is then tracked to keep a spectral line centred in a specified channel. The general relation between the radial velocity V_{rad}, the emitting frequency and the observed frequency is

given by $V_{rad} = c\frac{\nu_0^2 - \nu^2}{\nu_0^2 + \nu^2}$, where c is the speed of light. This formula is relativistically correct but approximations for V_{rad}<<c are commonly used. It is important to note that there are two definitions - radio and optical – resulting from these approximations. In the radio velocity definition the approximation is made directly with frequencies, giving $V_{radio} = c\frac{\nu_o - \nu}{\nu_o}$. In the optical velocity definition the frequencies are replaced with wavelengths and the approximation is then made, giving $V_{opt} = c\frac{\lambda - \lambda_o}{\lambda_o} = c\frac{\nu_o - \nu}{\nu} \equiv z$. Both velocity systems are used, with the optical definition being more common. Let's use a practical example. In the case of a galaxy with redshift z=0.045 and $V_{\rm hel}$= 13500 km s^{-1}, the central frequency will have to be set to 1359.2 MHz. Of course, as for every line observation, care should be taken to make sure the frequency of the redshifted line is in the tunable range of the receiver. Not all telescopes cover exactly the same range of frequencies. For example, in the case of the Westerbork Synthesis Radio Telescope, the sensitive L-band receiver covers frequencies up to 1160 MHz, corresponding to redshift z=0.22. For higher redshift, un-cooled receivers are available, resulting in an higher system temperature and, therefore, much lower sensitivity.

2.2 Bandwidth

The bandwidth required for HI observations depends on the project and on the possibilities allowed by the correlators of the different radio telescopes. In most projects, the total bandwidth is chosen to allow a large number of line-free channels on each side of the expected emission or absorption HI line. These channels are used to detect the continuum radiation so it can be subtracted, leaving only the line signal. The bandwidth available for spectral line observations is different depending on the capability of the correlator for the different radio telescopes. To take again the example of the WSRT, the band that can be set ranges from fraction of MHz (0.15 MHz) for high velocity resolution studies, up to 20 MHz. To have an idea of what this implies in term of velocity coverage, we can take a typical bandwidth of 10 MHz. In the case of the object that we proposed to observe in the previous section, this band will correspond to a range in frequency from 1354.2 to 1364.2 MHz (1359.2 MHz was our central frequency). In velocity, this covers from 12358 to 14665 km s^{-1}. Thus, with a 10MHz bandwidth we cover about 2300 km s^{-1}. This is usually a very good range for typical extragalactic studies. However, if we expect some extreme kinematics in the HI of our target objects or if we are interested in sampling a larger volume around the target object, we can also expand the bandwidth to the 20MHz band that will then correspond to 4600 km s^{-1}.

2.3 Velocity resolution

The choice of the channel width comes often from a compromise between the desired velocity resolution and the sensitivity needed. A detection experiment requires to match the channel width with the expected width of the line. Thus, in some cases relatively wide channels are necessary. Follow up observations to study in detail the kinematics of the gas, require higher velocity resolution. If we take some examples of HI in extragalactic objects, the typical velocity range observed goes from a few km s^{-1} in High Velocity Clouds, to ~100-400 km s^{-1} respectively for small and large galaxies, to 400-500 km s^{-1} for interacting systems and finally up to 2000 km s^{-1} for fast HI outflows detected in some powerful radio loud active nuclei. The choice of velocity resolution of the observations depends, therefore, on which kind of object are we interested in.

The channel width is given by $c\frac{\Delta v}{v_0}$ and this corresponds roughly (and for low heliocentric velocities) to 200 km s^{-1} for 1 MHz of channel width. Again for the case of the WSRT, the number of channels available goes from 64 to 1024 (2048 under certain conditions). Thus, for the 10 MHz bandwidth that we have considered above, 512 channels (quite typical for an extragalactic observation) would result in a width of the channel is 0.02 MHz and a velocity resolution of ~4 km s^{-1}.

One should not forget, though, that in some cases the velocity resolution needs to be degraded in order to remove effects due to the sharp changes in frequency spectrum - *Gibbs phenomenon* – via a tapering of the data. This phenomenon is due to the truncated nature of the temporal cross-correlation measurements in the spectrometer. The tapering of the data usually gets done via an Hanning smoothing. The Hanning filter can de applied either while observing or (even better) during the data reduction.

2.4 Sensitivity and spatial resolution

The sensitive of the observations (i.e. the r.m.s. noise per channel that can be reached) determine the column density of the gas that can be detected. One should consider that if a large array is used, its synthesized beam (i.e. resolution of the observations) will be small and as consequence the surface brightness sensitivity is reduced. This means that more observing time is needed to detect a given column density. This is particularly important to consider for HI emission that very often is distributed in large, low column density structures. Thus, one needs to be aware of what is the higher resolution where it is reasonable to expect for an HI detection, given the typical value for HI column density of known galaxies. Using the formula in Sec 1.1 we can derive the column density that we can reach for HI observations done with a certain spatial resolution. For example: if we observe with 5 arcsec resolution, with a velocity resolution of dV~ 30 km s^{-1} and we can reach an r.m.s. noise (per channel) of 1 mJy $beam^{-1}$, the resulting column density is $4x10^{21}$ cm^{-2} (at 1σ level). As mention above, this corresponds to the peak of column density seen in spiral galaxies. Thus, this resolution is too high to detect extended HI considering the typical sensitivity that can be reached with the available radio telescopes! If we observe at much lower resolution, e.g. 60 arcsec, we can detect HI emission

with a column density of 2.8 x10^{19} cm^{-2} and this will more likely provide a detection of faint extended HI.

It is worth noting that this is not the case for absorption. As shown in the formula in Sec. 1.2 the column density depends on the optical depth, so, to a first order, on the ratio between the absorbed flux and the underlying continuum flux. The stronger the continuum source is, the lower is the column density that can be probed.

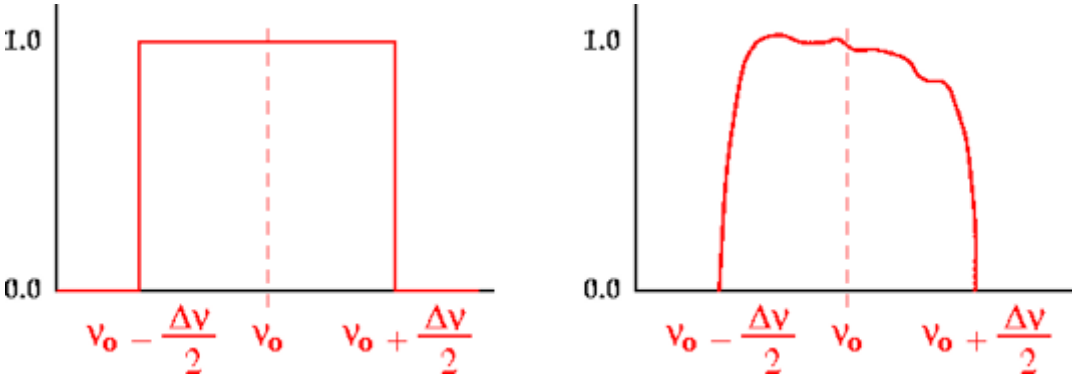

Figure 2 - Sketch of the "ideal" bandpass (left) and how it may look in real life (right) (from J. Hibbard, NRAO Lecture)

3. How to carry out the observations

3.1 Calibrating the data: the bandpass

For line observations (and for continuum observations done in spectral-line mode) calibration of the antenna-based bandpass function is needed. The shape of the bandpass is due primarily to electronics and transmission systems individual antenna and varies for every antenna. As shown in Fig. 2 the shape of the bandpass can be quite complex.

Usually for spectral line observations carried out with an interferometer, this calibration is done by observing a strong calibrator. Care must be taken if strong continuum sources are present in the field. Depending how accurate the calibration of the bandpass has to be, one may need to observe a *strong* calibrator few times during the observations: this allows to follow possible variations of the bandpass with time. However, in general the variation with time are much slower than atmospheric gain or phase terms.

The shape of the band is corrected using a source with known characteristics as illustrated in Fig. 3. After this step (and the gain correction) the dataset is ready for being imaged following the same procedure as described e.g. in the lecture of D. Dallacasa. However, in the case of line observations every channel will provide one image that will form a data cube (as illustrated in Fig. 4).

The structure of a data cube is three axes associated with right ascension, declination and a third axis associated with frequency or radial velocity. A typical data cube has therefore 256 or 512 pixels in the RA and DEC axes and as many pixels in the frequency/velocity as the channels to be imaged.

3.2 Continuum subtraction basic concepts

The data cube obtained from the Fourier Transform of the calibrated data will include the signal from both the line and the continuum emission. As illustrated in Fig. 4 (and for definition of line emission!) the intensity of the line does depend on the frequency while the continuum covers the entire band (at most changing in intensity due to spectral index effects). Depending on the nature of the target source, the continuum can varies from being very strong and the dominant signal (for radio loud galaxies), to very weak or absent (e.g. for radio quiet objects). The two components (line and continuum) need to be separated in order to analyse the line emission (or absorption) alone.

There are two main methods to subtract the continuum. In either case, one needs to use the channels without line emission, model the continuum there and subtract it from the dataset or the datacube. If the continuum is particularly strong and/or the line emission particularly weak, this process results in an iterative process where the main game is to identify the channels that really are line-free!

The continuum can be subtracted in the ***uv*-plane.** A fit of the line-free channels of each visibility is performed using a low-order polynomial. The fit is then subtracted from the data before mapping**.**

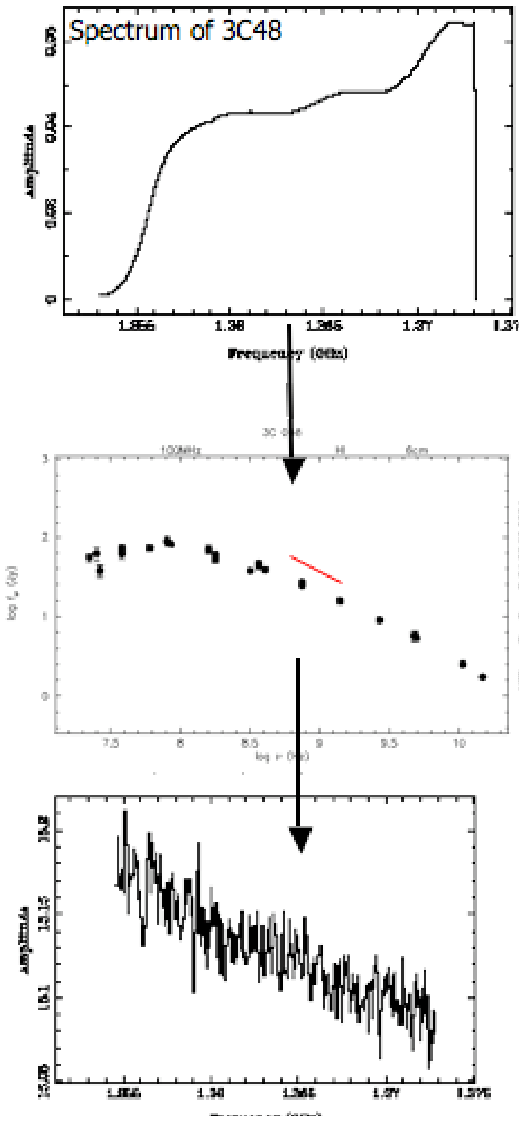

Figure 3- The shape of the bandpass for WSRT observations of 3C48 (top). Bandpass after the correction (botton). The slope represents the real effect of the spectral index of the calibrator.

The continuum can also be subtracted in the **image plane.** In this case, one should first image the data (build the datacube) and then (again) use the line-free channels in each pixel of the spectral line data cube and fit them with a low-order polynomial and subtract the continuum emission.

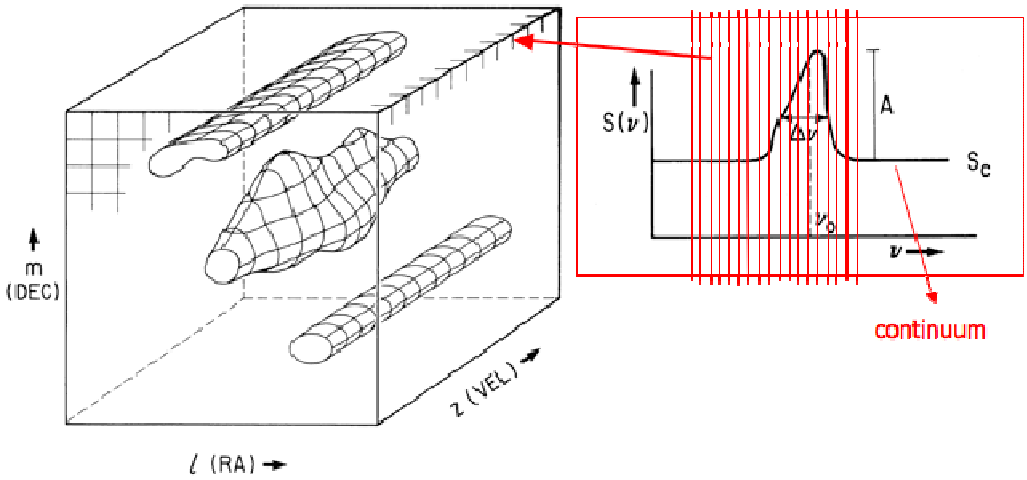

Figure 4 - Sketch of the resulting data cube (from [4])

3.3 Looking at HI data

A data cube can be explored in different ways. Software is available to look e.g. at a movie of the data but for publication or display purpose, 2-D visualisation of the data are also needed.

Playing a movie of the data-cube means to go through the images in the cube at high enough speed to be able to see the signal (if any!) "moving" through the cube. Examples of movie of data cubes can be found in the on-line version of this presentation. The movie can be played by looking at RA-Dec images for different velocities (i.e. channels) but the cube can also be inspected by looking at e.g. RA-Vel changing through declinations planes. Different movies can be used to show different structures of the emission (of absorption). One can also produce a volume rendering of the HI emission/absorption in the cube. The 3D visualisation tools are usually very powerful to identify structures or weak emission/absorption.

As mentioned above, although spectral line maps are inherently 3-dimensional, some methods are required to visualize the data on paper and to be able to publish the results. There are few examples of these methods.

- *1-D Slices along velocity axis*: this gives line profiles (see Fig.5);
- *2-D slices along velocity axis* can be made, in other words images of the channel maps can be presented. These are contours or grey/colour scale plot of each

channel (or of a representative group of channels). For some examples see e.g. [8].

- The 2-D plots can also be made along a *spatial dimension* e.g. the major axis of the galaxy. These are the so-called position-velocity plots of the distribution of the HI. An example is shown in Figs. 6 and 7.

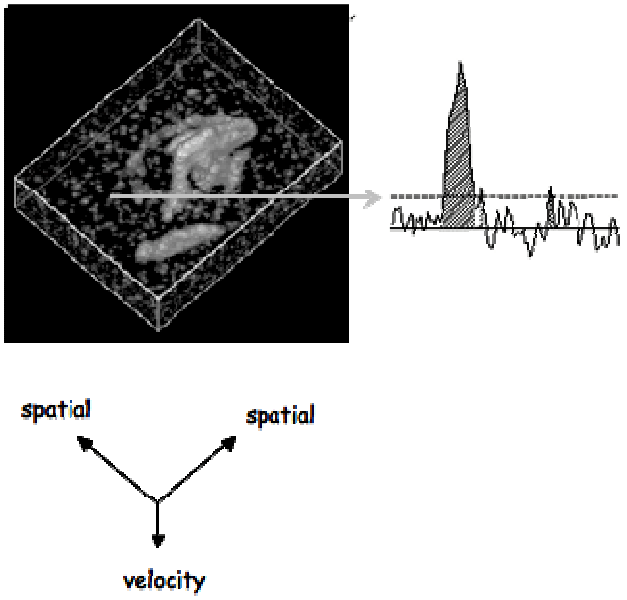

Figure 5- Example of 1D slice through a complicated data cube (NGC 4631, courtesy of T. Oosterloo)

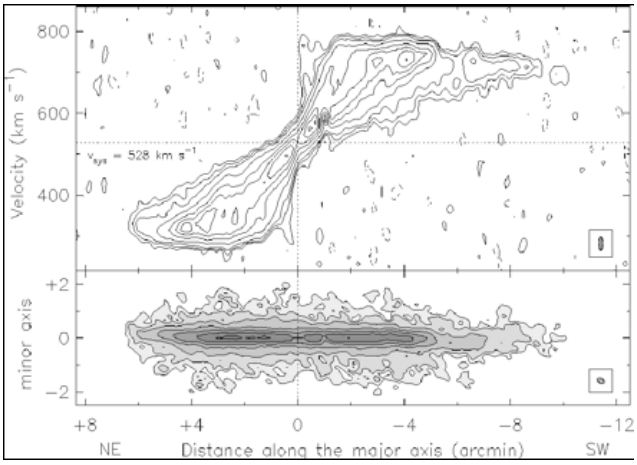

Figure 6 - Position-velocity plot of the HI along the major (top) and minor (bottom) axis of the galaxy NGC 891 (Credit: Swaters, Sancisi, van der Hulst 1997).

Another common way to display HI results is via images representing the integral properties of the line emission/absorption (integrals over velocity).

The ***0th moment*** represents the integrated flux, i.e. the intensity integrated over all channels with HI detected: $N_{HI}(RA,Dec) = \Delta v \sum_{i=1}^{n_{tot}} I_i(RA,Dec)$

The ***1st moment*** represents the intensity weighted mean velocity: $\bar{v} = \frac{\sum_{i=1}^{n_{tot}} I_i(RA,Dec) v_i}{\sum_{i=1}^{n_{tot}} I_i(RA,Dec)}$

Finally, the ***2nd moment*** represents the intensity weighted velocity dispersion.

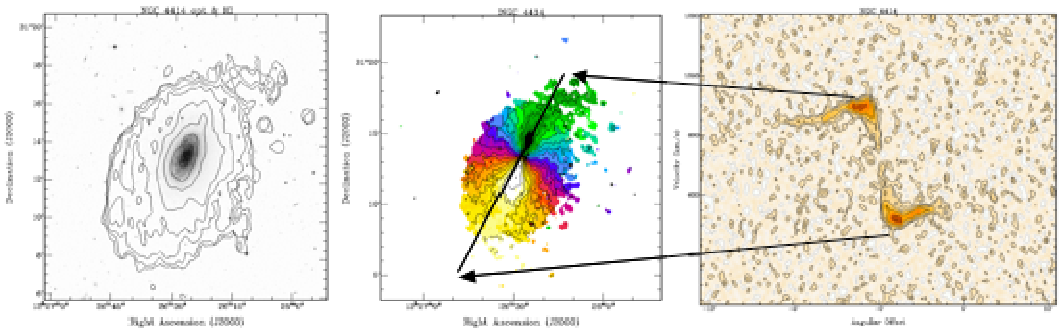

Figure 7 - Total HI intensity (left) superimposed to the optical image of NGC443 (courtesy T. Oosterloo). The central image represents an HI velocity field (yellow part representing receding gas while the green part is approaching gas). A 2-D position velocity diagram taken along the major axis of the galaxy is shown in the right image.

The result is to collapse the frequency dimension and produce one image for each of the moments. To illustrate some of the results from the moment analysis, Fig. 7 shows the distribution of the neutral hydrogen in the galaxy NGC 4414. The left image has the contours of the total HI distribution superimposed onto an optical image while the velocity field is shown in the central image.

As further example, Fig.8 represents the total intensity of NGC 4631 (the galaxy shown in Fig. 5). The structure of the HI is clearly very messy as expected in the case of a galaxy strongly interacting. For comparison, the optical image of the field is shown. It is clear that the HI is crucial to get a full picture of what is happening to this object.

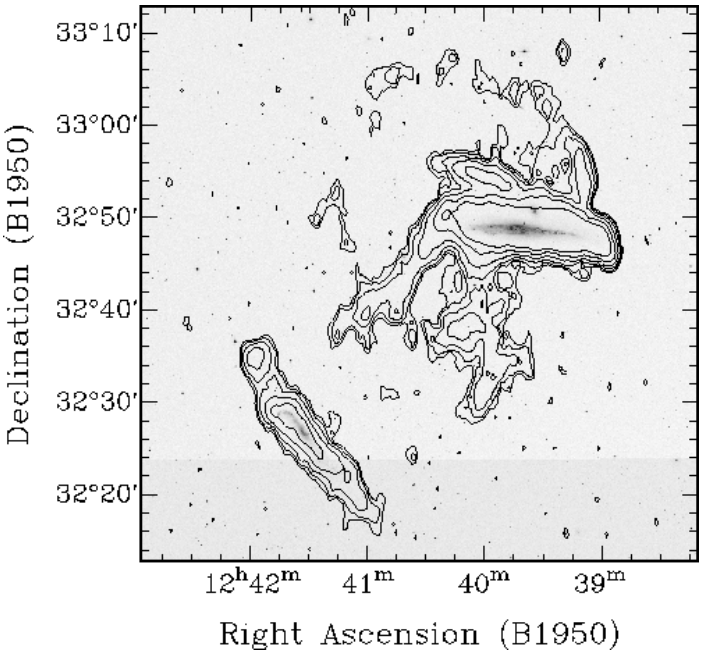

Figure 8 - Left: An example of HI detected in the interacting system, NGC 4631 (upper galaxy) and NGC 4656 (lower galaxy), see also Fig. 5. The HI total intensity (contours) is superimposed onto an optical image of the same field. This shows how different and more regular the distribution of stars appears compared to the emission from the neutral hydrogen. The data were obtained with the Westerbork Synthesis Radio Telescope (regions with more contours correspond to a stronger emission). The large tails of gas between the interacting galaxies are clearly visible (Courtesy of T.A. Oosterloo and K. Kovac, ASTRON/RUG)

4. Examples of studies of associated HI

It is impossible to cover in such a short paper all topics where the study of the neutral hydrogen is or has been relevant. Therefore, I will just briefly touch upon some results related to the study of galaxy formation and evolution.

4.1 Our Galaxy and surrounding

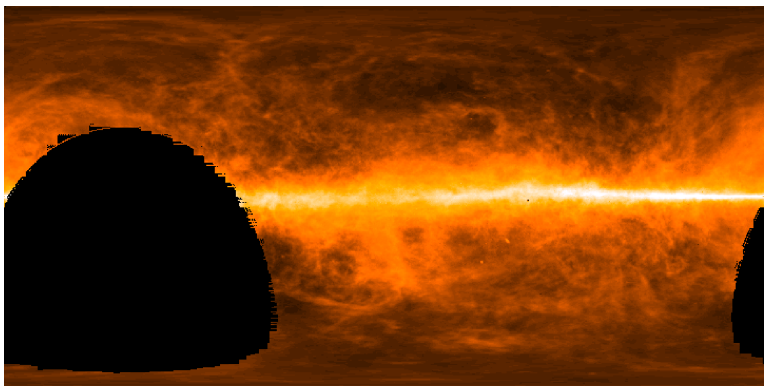

Figure 9 – All-sky image of the HI column density from the Dwingeloo-Leiden survey [2].

Observations in 21-cm HI line have yielded quite detailed maps of the distribution of cooler component of the interstellar medium (ISM) in many galaxies. The first object studied was, of course, our own Milky Way. Approximately 5 – 10 % of the mass of the Milky Way is

in the form of interstellar atomic hydrogen. Although insight into the structure of our Galaxy can be sought in a number of different ways, the study of the neutral hydrogen is particularly suited. The 21-cm profiles can be interpreted to give information about differential galactic rotation. Fig 9 shows the all-sky column density distribution of neutral hydrogen with the plane of our Milky Way Galaxy running horizontally through the centre. The gas is organized into diffuse clouds and dust that have sizes of up to hundreds of light years across and which tend to cluster near the plane of the Galaxy. Most of the image is based on the Leiden-Dwingeloo Survey of Galactic Neutral Hydrogen. This survey was conducted over a period of 4 years using the Dwingeloo 25-m radio telescope.

Also using the old Dwingeloo telescope, it was discovered already more than four decades ago, by Muller, Oort and Raimond, that our own Milky Way galaxy has a large population of clouds of neutral hydrogen, the so-called High-Velocity Clouds (HVCs), whose location and kinematics indicate that they are located in the Galaxy's halo or beyond.

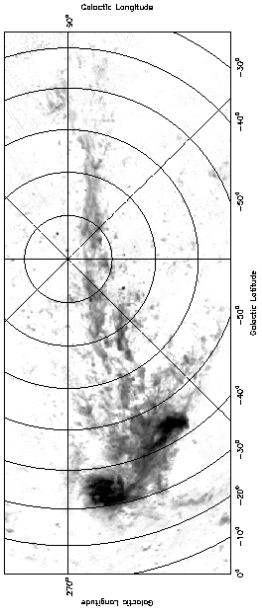

Figure 10 - Image of the distribution of the neutral hydrogen in the Magellanic Stream (taken from [4]). Darker regions represent zones where the signal is more intense. The two dark clouds correspond to the Magellanic Clouds connected by a bridge of neutral hydrogen. The tail going up from these Clouds is the Magellanic Stream. The Milky Way is just outside the figure at the bottom.

Our galaxy also represents the closest example of galaxy interacting with its neighbours. A giant stellar stream surrounds the Galaxy and it is originated by a companion dwarf galaxy, the Sagittarious dwarf. Furthermore, a narrow tail of neutral hydrogen, the so-called Magellanic Stream is already known for many years. This stream trails the (Small and Large) Magellanic Clouds - the two closest companions of the Milky Way - along a circle around the Milky Way. More recent studies with the Parkes radio telescope in Australia, have shown that this stream of neutral hydrogen is much more extended than previously thought, as it extends also in a direction opposite to what known so far (see. Fig.10). Astronomers consider this a further confirmation of the idea of tidal interaction between the Magellanic Clouds and the Milky Way. This means that slowly the Magellanic Clouds will be torn apart and destroyed and their gas and stars will become part of the Galaxy.

4.2 Nearby galaxies, gas accretion and dark matter

Fig. 11 shows a nice image of the HI distribution in the nearby galaxy NGC6946. The image shows how the HI follows the spiral arms but it also shows how clumpy the distribution is. Large holes, possibly originating by supernova explosions, are also clearly visible. The large

distribution of the neutral hydrogen - compared to the stellar distribution - has been and still is crucial in the discovery and study of dark matter in galaxies.

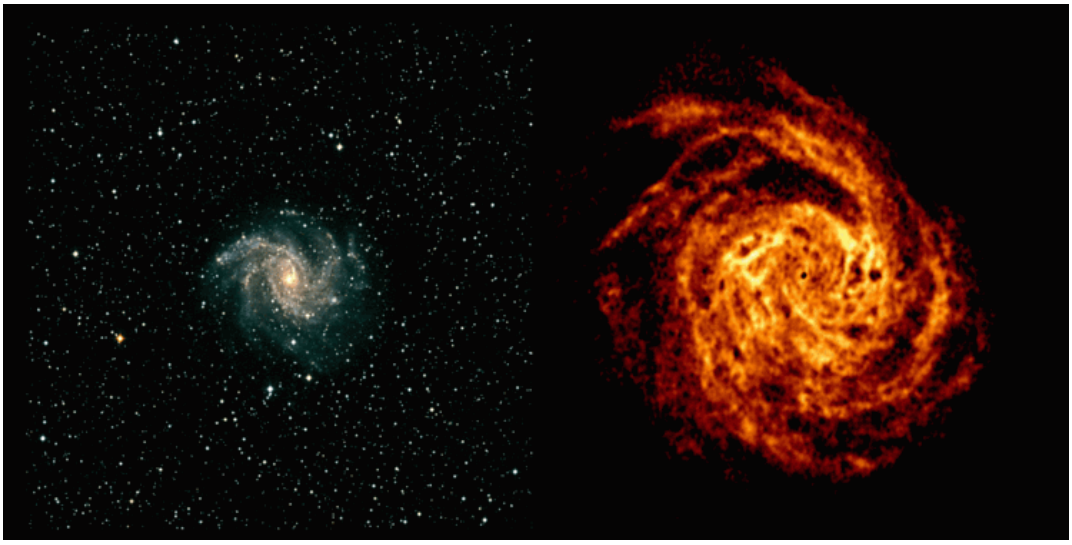

Figure 11 - The almost face-on spiral galaxy NGC 6946. On the left, a true colour optical image (base on images from the Digital Sky Survey) is shown while on the right a deep image of the neutral hydrogen obtained with the Westerbork Synthesis Radio Telescope revels how much extended is the gas compared to the stars. (Credit: R. Boonsma & T. Oosterloo, RUG/ASTRON)

In addition to the gas closed to the galactic plane and following the spiral arms, gas clouds seem to form arching and looping structures away from the plane, possibly stirred up by stellar activity in the galactic disk. The existence of such cold, gaseous halos in spiral galaxies is not entirely surprising. It would be natural to assume that other spiral galaxies have a population of HVCs similar to what our Milky Way has. However, only recently, due to the improved performance of radio telescopes, it has become feasible to actually detect such extragalactic HVCs.

Exciting results have been obtained for the edge-on galaxy NGC 891 where about 10% of the halo detected is in the form of gas clouds and filaments. The most striking example of this anomalous gas is a large filament 20 kpc long and extending to the NW, almost perpendicular to the disk (see Fig. 12). While such deep observations will hopefully become "routine" once SKA will be available, at the moment they represents one of the deepest HI observations available for a nearby galaxy. Two main explanations have been offered for the existence of the H I halos and their structures. One is the so-called *galactic fountain* in which star formation and stellar winds drive flows of gas from the disk into the halo. The second kind of model explains the gaseous halo by accretion, either of small, gas-rich companions, or of gas clouds directly from the intergalactic medium (also known as Oort's *cosmic drizzle*). The observations of NGC 891 indicate that both mechanisms operate in this galaxy. The gas that is regularly rotating in the lower halo is most likely gas brought into the halo by star formation, as proposed in the galactic fountain model.

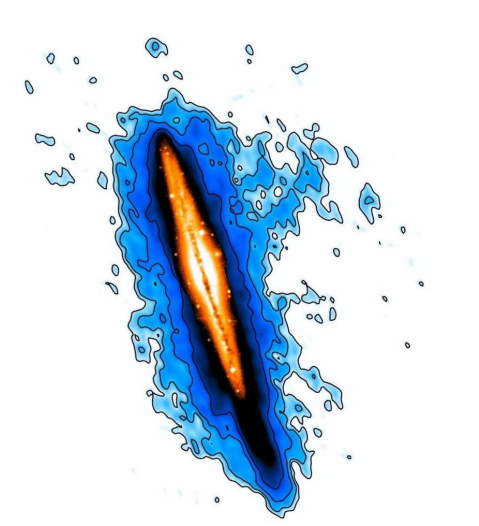

Figure 12 - Rendering of the H I halo (blue) detected in NGC 891. The orange inset shows the edge-on optical image of the galaxy. Gas filaments and clouds are found up to more than 20 kpc from the disk (from Oosterloo et al. 2007).

4.3 Interacting systems

The most impressive galaxy mergers are those between two galaxies of similar size (so-called major mergers). The system known as The Antennae represents one of the most amazing cases and Fig.13 shows the extremely complex structure in all details. The system consists of the collision of two galaxies and the striking features of the picture are the two huge "antennae" that represent gas and stars pulled out of the galaxies during the encounter. Numerical simulations show that these structures are indeed the result of such an encounter *if* the galaxies passed by each other in the same sense as the rotation of each disk of stars (so-called prograde encounter). In this case, the outer rings of stars and gas are ripped off from each of the galaxies, resulting in the formation of the spectacular tails.

There are many cases known of major mergers and, by studying their characteristics, it has been possible to construct a sort of evolutionary sequence. For example, the Antennae still show the two separate bodies of the merging galaxies and prominent tails of stars and gas. Large quantities (many times our Galaxy) of neutral hydrogen are observed from the centre of the merger to the end of the tails. This merger likely started a few hundred million years ago.
Finally, we should not forget that the distribution of the gas at large scale is also very sensitive to the environment where galaxies reside. Clear indications of gas stripping have been found using deep HI observations of galaxy in clusters.

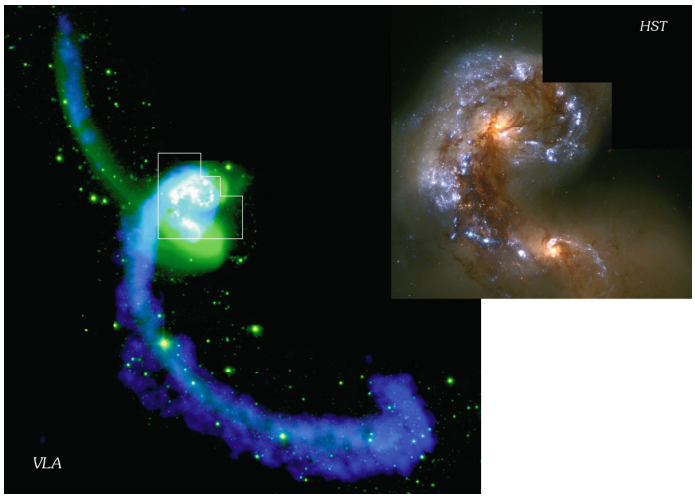

Figure 13 - The two colliding galaxies known as Antennae. The figure on the left shows the neutral hydrogen in blue (from observations with the NRAO Very Large Array) superimposed on an optical image from the CTIO 0.9m in green and white. This image clearly shows the long tails created by the interaction. The image on the right shows the centre of the two interacting galaxies as observed by HST. (Credit: NRAO/AUI and STScI/NASA, investigators Hibbard J.E., van der Hulst J.M., Barnes

J.E., Rich – Whitmode B. & Schweizer F.; taken from www.nrao.edu/imagegallery)

4.4 Gas and Active Galactic Nuclei (AGN)

As discussed above, atomic neutral hydrogen can also be detected in absorption against a strong continuum source. This is quite commonly seen against the central regions of radio galaxies. An example is shown in Fig. 14 . Such narrow absorptions (FWHM ~ 100-200 km s^{-1}) are often considered to be the result of the presence of a circum-nuclear disk.

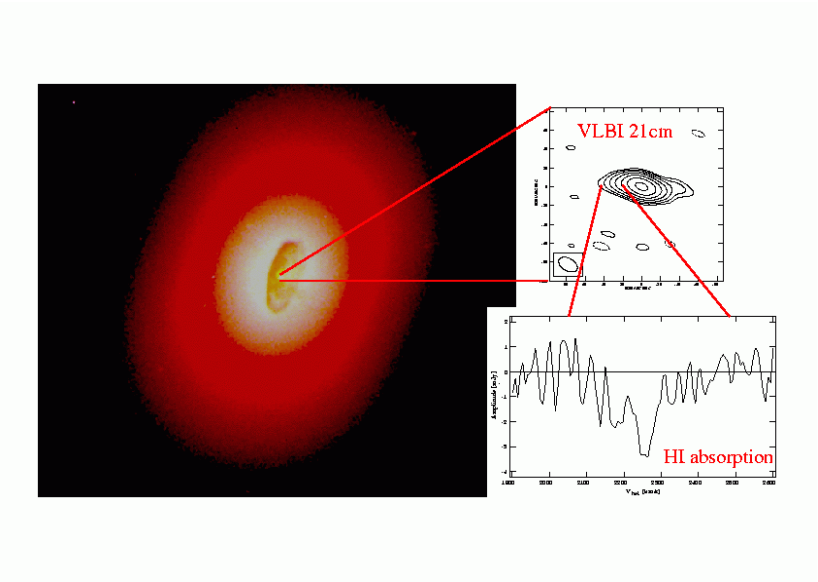

Figure 14 - Example of HI absorption against the nuclear region of a radio galaxy (Courtesy of H.J. van Langevelde). On the left is an HST image of the central region of the radio galaxy NGC4261. On the top-right is the continuum image and bottom-right the HI absorption observed against the continuum [12].

However, thanks to deep HI absorption it is also clear that the medium around AGN can be kinematically more complex than this, i.e. not all the gas is settled in regularly rotating structures. Fig. 15 shows how the HI absorption looks when very deep observations are obtained (with the WSRT) for the powerful radio galaxy 3C293 [4]. In addition to the deep HI absorption - located close to the systemic velocity of the galaxy - likely originating from a circum-nuclear disk, a very broad and shallow absorption has also been observed. The width (full width at zero intensity) of the absorption reaches ~1400 km s^{-1}, one of the broadest found so far in HI 21-cm absorption in any class of astronomical objects. Similar broad HI absorptions have been found in other powerful radio galaxies and in all cases most of the absorption is *blueshited* compared to the systemic, unambiguously indicating that the gas is part of a fast outflow.

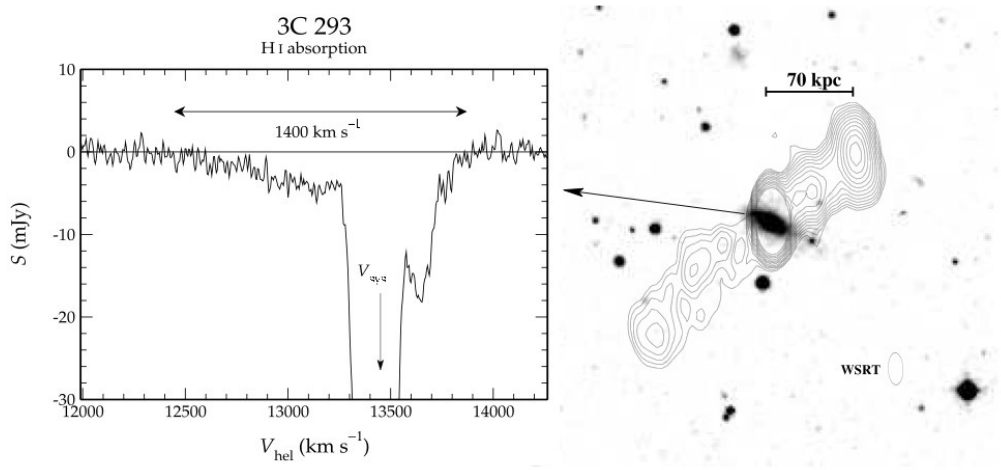

Figure 15 - Radio continuum of the radio galaxy 3C293 (right) superimposed onto an optical image. Left: HI absorption detected against the nucleus of the radio galaxy [4].

4.5 Intervening HI

Finally, the atomic hydrogen producing the absorption does not have to be only associated with the target galaxy but can also be located along the line of sight, i.e. between the radio source and us. An example of such absorption is shown in Fig. 16. They are usually associated with Damped Lyα (DLA) systems, high neutral column density ($N_{HI}>10^{20}$ cm^{-2}), possibly the progenitors of present days ordinary galaxies.

These kinds of HI absorption are quite rare and require observations of large areas of sky in order to build a statistically significant sample. In order to achieve this, new wide field systems are needed to make the speed at which large part of the sky can be surveyed much faster.

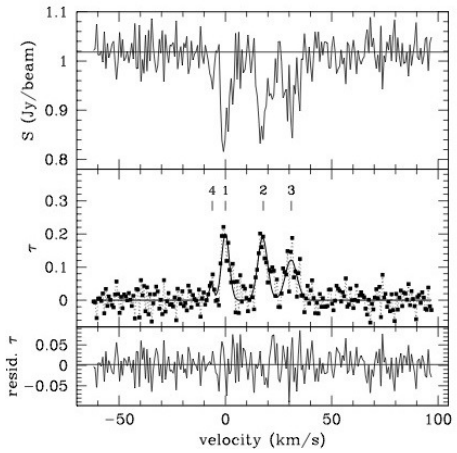

Figure 16 - Example of intervening absorption. WSRT spectrum of the z=0.3941 HI 21-cm absorber toward B0248+43(from [3]).

5. Going further ahead (toward SKA)

Some of the results presented above have been obtained only after extremely long observations with the best radio telescopes available at present. In a way, they represent the best we can do now! The future work on atomic neutral hydrogen will require a major step forward in the sensitivity of radio telescopes and for this we will need to wait until SKA will come on-

line. However, another aspect important for the improvement of present day telescopes, on the way to SKA, is the field of view. Many of the research topics in HI astronomy would substantially benefit from the possibility to perform deep observations that cover large areas in the sky, therefore resulting in the detection of many *interesting* objects in each observation.

Apart from using many small dishes to expand the field of view of an interferometer, other systems are at the moment experimented and, if successful, will provide a new technology for the SKA. Aperture array and focal plane array are both being considered. EMBRACE, part of the SKADS project, is one of such test for aperture arrays and is described in more detail in the lecture by F. Perini.

In a similar way, focal-plane arrays aim to substantially enlarge the field of view of reflector radio telescopes at decimeter wavelengths. One of such system, APERTIF, is planned to be installed in each dish of the WSRT, substantially increasing (25 times) the field-of–view of this telescope. With such a larger field of view, it becomes feasible to survey the entire sky on short timescales with high sensitivity and at high spatial resolution. This will enable entirely new types of astronomical research. For example, currently the H I properties are known for about 10,000 galaxies, mostly with a spatial resolution of several arcminutes and only a few dozen detections have a redshifts above 0.1. With a telescope like the WSRT equipped with focal-plane arrays one will be able to do an all-sky H I survey resulting in a database of about 1,000,000 galaxies, all imaged at 15 arcsec resolution and the large majority of the detections will have a redshift above 0.1.

The first prototype, DIGESTIF, is now installed in one of the WSRT telescope (see Fig. 17). The full system, called APERTIF, is planned to be installed in 2009.

Figure 17 - The DIGESTIF system (prototype of APERTIF) mounted on one of the WSRT dishes (courtesy of W. van Cappellen).

Acknowledgements

I would like to thank the organisers and in particular Franco Mantovani for putting together this enjoyable school. A big thanks goes to Tom Oosterloo for kindly providing some of the beautiful pictures shown in this paper and obtained from deep observations with the Westerbork Synthesis Radio Telescope.

References

[1] Bahcall, J. N., & Ekers, R. D. 1969, ApJ, 157, 1055

[2] Hartmann, Dap, Burton 1997, *Atlas of Galactic Neutral Hydrogen*, CUP ISBN 0-521-47111-7

[3] Lane W, Briggs F. 2001ApJ...561L..27 2002

[4] Morganti R., Oosterloo, T. A., Emonts, B. H. C., van der Hulst, J. M., Tadhunter, C. N. 2003 ApJ 593L, 69

[5] Oosterloo T., Fraternali F., Sancisi R., 2007 AJ 134, 1019

[6] Putman et al. 2003 ApJ 586, 170

[7] R. Perley, F. Schwab, A. Bridle, in *Synthesis Imaging in Radio Astronomy*, ASP Vol. 6

[8] Roelfema P. 1994, in *Synthesis Imaging in Radio Astronomy,* Perley R.A., Schwab F.R., Bridle A.H. eds., ASP Vol. 6, p. 315

[9] Spitzer L. 1968, *Diffuse Matter in Space* New York:Interscience

[10] Swaters R.A., Sancisi R., van der Hulst J.M., 1997, ApJ 491, 140

[11] Van Gorkom J.H., Ekers R.D. 1994, in *Synthesis Imaging in Radio Astronomy,* Perley R.A., Schwab F.R., Bridle A.H. eds., ASP Vol. 6, p. 341

[12] van Langevelde, H. J., Pihlström, Y. M., Conway, J. E., Jaffe, W., Schilizzi, R. T. 2000, A&A 354L, 45

[13] G. Verschuur, K. Kellerman, *Galactic and extra-galactic radio astronomy*, Springer-Verlag *1974*

[14] Westpfahl D.J., 1999, in *Synthesis Imaging in Radio Astronomy II*, Taylor G.B., Carilli C. & Perley R.A. ASP Vol. 180 p. 201

.